A Prominent Ionization Cone and Starburst Ring in the Nearby Circinus Galaxy

A. MARCONI[1], A.F.M. MOORWOOD[2], L. ORIGLIA[3] and E. OLIVA[4]

[1] *Dipartimento di Astronomia e Scienza dello Spazio, Università di Firenze, Italy;* [2] *ESO-Garching;*
[3] *Osservatorio Astronomico di Torino, Italy;* [4] *Osservatorio Astrofisico di Arcetri, Firenze, Italy*

Introduction

The characteristic spectra of Seyfert nuclei have long been generally attributed to photoionization by the hard UV continuum of a central black hole and associated accretion disk. More recently, within the context of AGN unification schemes, it has been proposed that the primary difference between Seyferts of type 1 and 2, i.e the broad permitted lines seen in the former, could be attributed to the presence of an obscuring torus in which case visibility of the nucleus depends on viewing angle. Supporting evidence has come from the detection of 'hidden' BLR's in reflected polarized, light and of ionization cones which imply some 'collimation' of the nuclear UV continuum (c.f Antonucci 1993 for a review). Also of interest in the context of unification
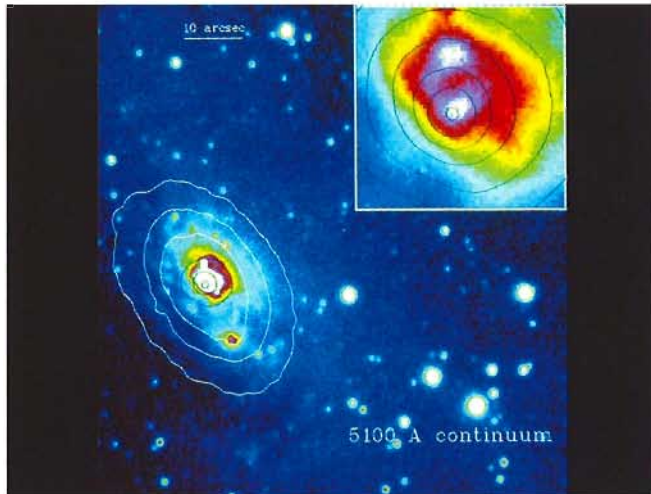

Figure 1: *SUSI image of the Circinus galaxy in the 5100 Å continuum. N is at the top and E to the left. The 10" scale bar applies to the large image and the insert shows the nuclear region enlarged by a factor 5. The contours are from the K'(2.1 μm) image. Note the double nucleus at 5100 Å and the displacement of the K' peak relative to the southern component.*
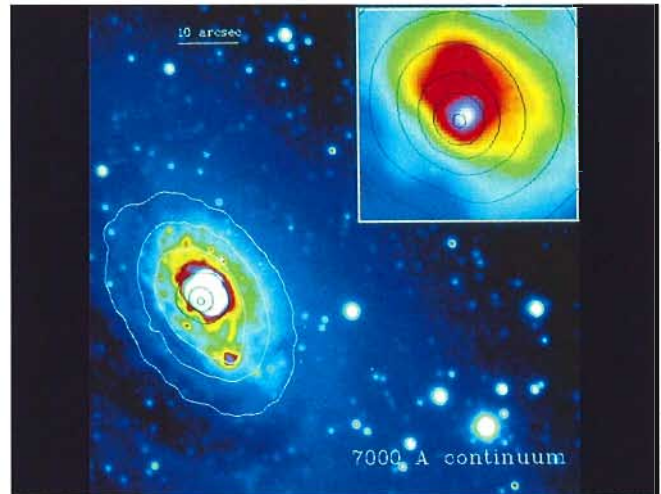

Figure 2: *Same as Figure 1 at 7000 Å. Note that only the southern 'nucleus' is visible.*
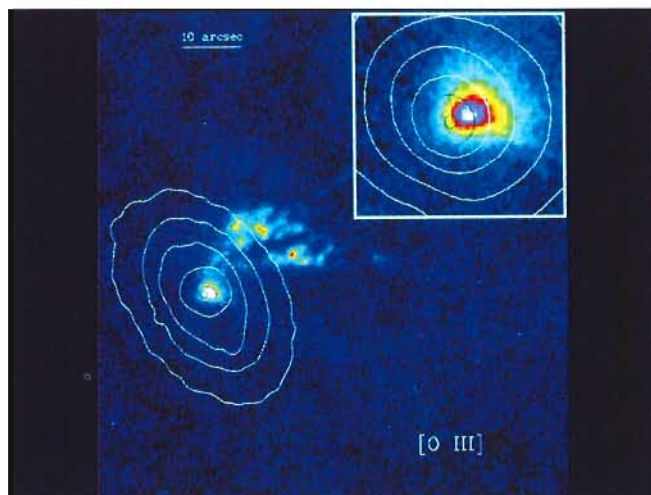

Figure 3: *Same as Figure 1 but in the [OIII] line. Note the clear cone-shaped structure and the displacement between the line and K' continuum peaks.*
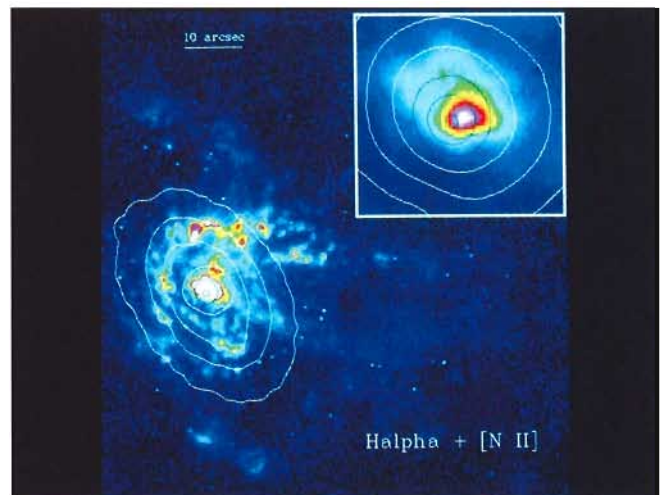

Figure 4: *Same as Figure 1 but in the Hα + [NII] which reveals a partial starburst ring.*
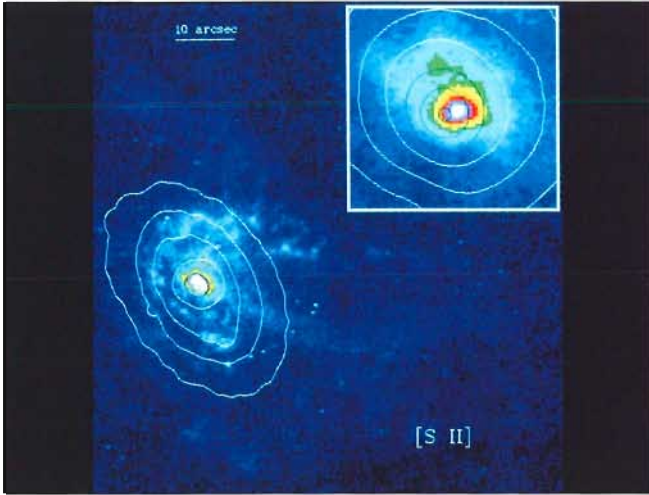
Figure 5: *Same as Figure 1 but in the [SII] line. Note the remarkable chain of spots in the SW which are probably supernova remnants.*
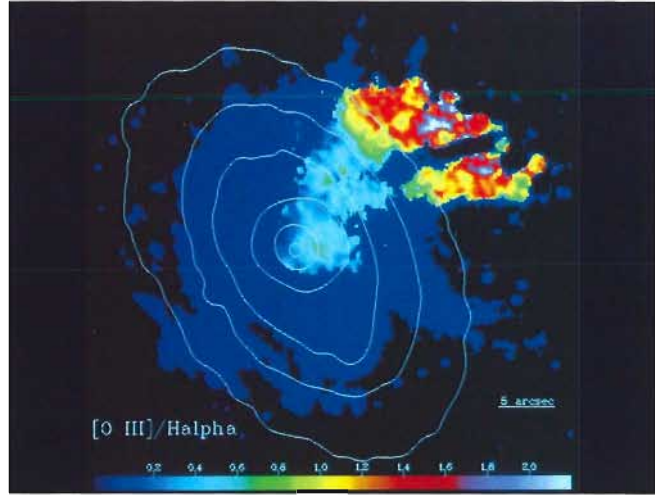

Figure 6: *[OIII]/(Hα+[NII]) showing the ionization structure of the cone. The uniform dark blue region is where Hα+[NII] but not [OIII] was detected at more than 10σ.*

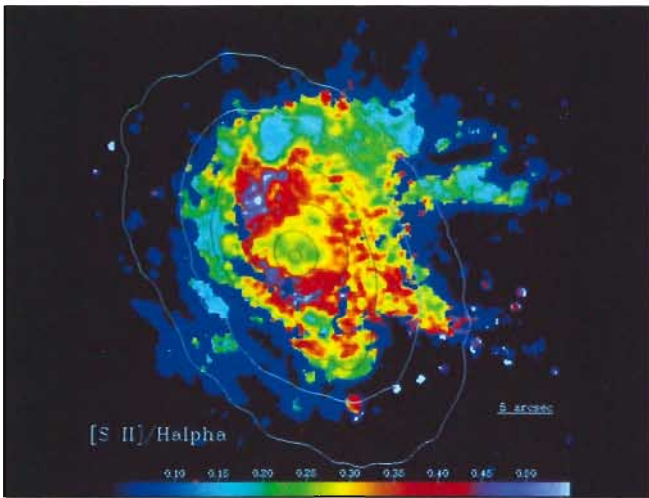Figure 7: *Same as Figure 6 for [SII]/Hα. The chain of spots in the SW believed to be supernova remnants are particularly obvious.*

is the evidence for circumnuclear starbursts in many Seyferts which may be only circumstantially associated with the AGN activity but could also be consistent with suggestions that the central black hole forms and/or is fuelled by the remnants of a precursor starburst.

In the Circinus galaxy, at a distance of only 4 Mpc, we believe we have discovered the closest example of a Seyfert galaxy showing both a prominent ionization cone and a circumnuclear starburst ring. Circinus is a spiral galaxy of uncertain type which lies close to the galactic plane and whose IRAS infrared luminosity is a moderate 10^{10} L$_\odot$. Evidence for Seyfert activity is provided by its large [NII]/Hα ratio and, more compellingly, by its extremely prominent visible and infrared coronal lines from ions with ionization energies up to 300 eV (Oliva et al. 1994, hereafter O94) including [SiIX](3.95 μm, 303 eV) and [SIX](1.26 μm, 323 eV) detected for the first time.

In order to further investigate the nature of this galaxy within the above con-

text we have obtained both line ([OIII], Hα + [NII], [SII], [FeXI]) and continuum (5100, 7000 Å, J(1.25 μm), H(1.65), K'(2.1)) images using SUSI at the NTT and IRAC2 at the 2.2-m telescope on La Silla. Our purpose here is to describe the observations and show the results which, because of the closeness of this galaxy, provide very striking examples of an ionization cone and circumnuclear starburst. A more detailed analysis, including the modelling referred to below, will be published in a forthcoming paper.

Observations

Optical line and continuum images were obtained in April 1993 with SUSI at the NTT. Seeing which was both good ($\simeq 0.7''$) and stable for several hours contributed to obtaining a satisfactory subtraction of background stars in the final line images. The filters employed were ESO #700 ([SII]), #629 (Hα+[NII]), #369 ([OIII]), #430 (5100 Å continuum), #443 (7000 Å continuum) and #415 ([FeXI]λ7892). More details on

the ESO filters (including transmission curves) can be found within MIDAS using the command CREA/GUI FILTER.

In each filter we took several short (15 min) integrations with the object at different positions on the CCD. The images were then flat-fielded, dark-subtracted, realigned and stack together using AVERAGE/IMAGE which also removed cosmic-ray events (using the 'median option'). The resulting frames were then sky subtracted and flux calibrated following standard procedures.

The most difficult part of the reduction was the continuum subtraction. The galaxy lies close to the galactic plane in a field crowded with foreground stars of different colours (Figs. 1, 2) and, within the galaxy itself, there are large colour variations caused by patchy extinction (e.g. a dust lane) and different stellar populations (e.g. a bluer starburst in the central few arcsec). A straight line–continuum (e.g. Hα–7000 Å) image subtraction produced negative regions corresponding to red objects (including the compact nucleus of the galaxy) while blue objects left a positive residual. This problem was overcome by creating artificial continuum images at the line wavelengths using a power law interpolation between continuum frames at shorter and longer wavelengths. This gave satisfactory results for all line images except [FeXI] whose underlying continuum (at $\lambda \simeq 8000$ Å) could not be accurately reproduced by extrapolation from 7000 Å (the reddest continuum point) while a suitable longer wavelength filter could not be simultaneously mounted in SUSI for technical reasons. Adding the J (1.25 μm) IR broad band image provided a partial solution but at the cost of decreased image quality (the IR image was taken under poorer seeing conditions).

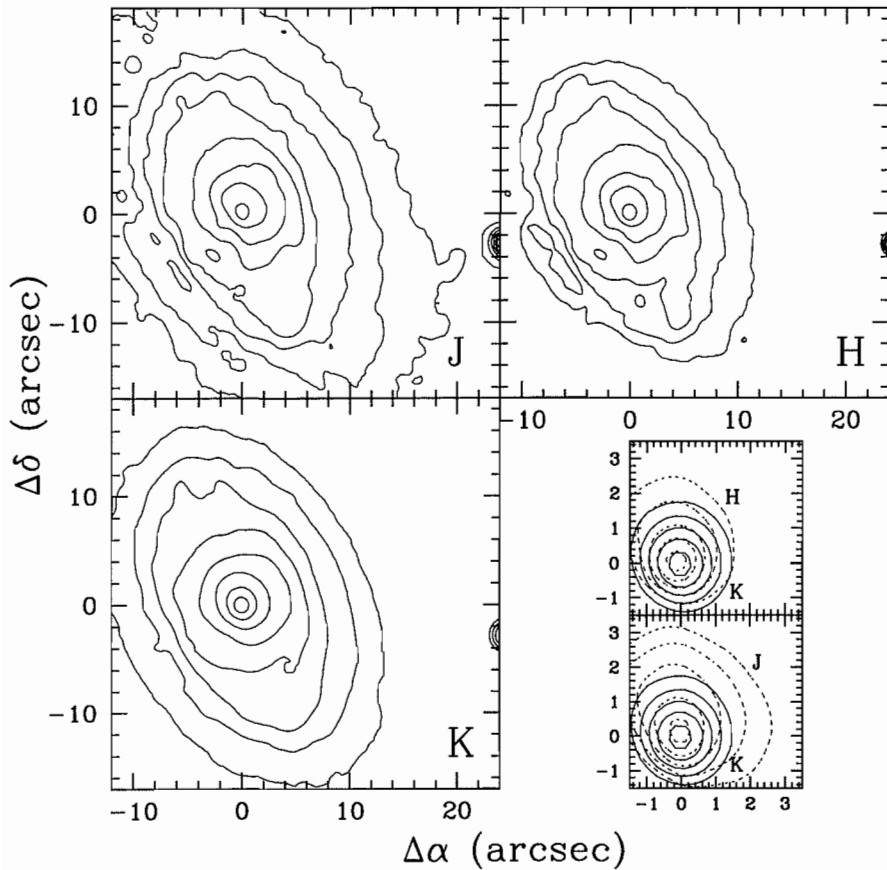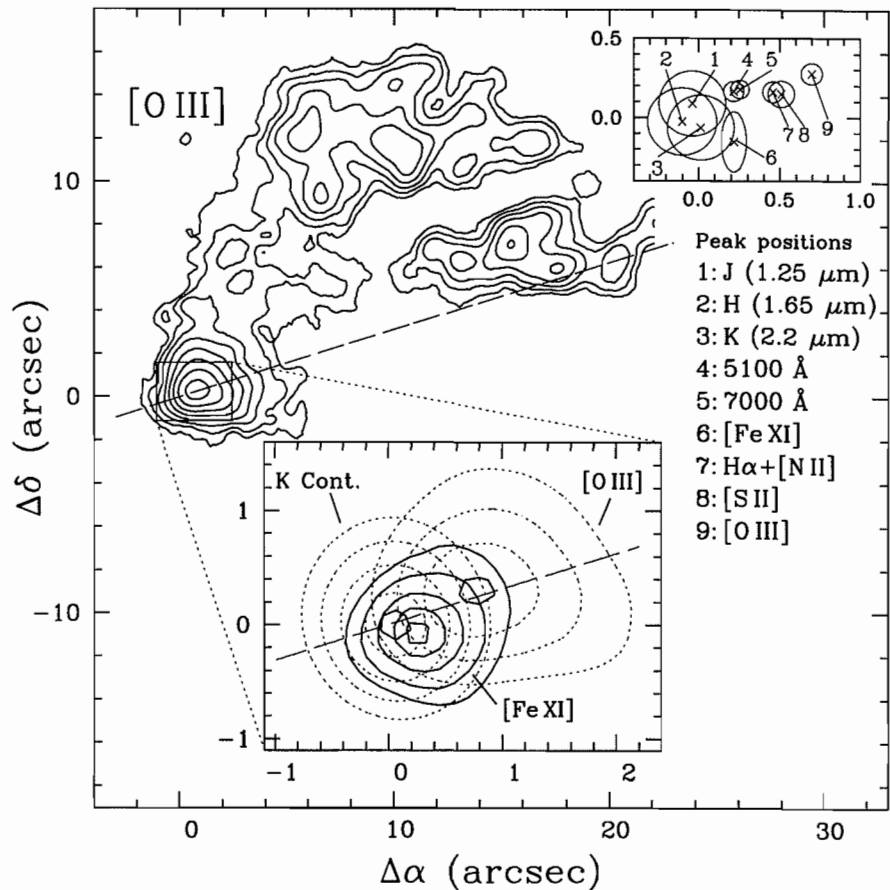The IR images were obtained with the IRAC2 camera at the ESO/MPI 2.2-m

Figure 8: *Contour plots from the IRAC2 J, H and K' images. The insert shows an increase in compactness with increasing wavelength but no relative displacements (within the uncertainties) of the single nuclear peak.*

ground stars) and subtracted from the object frames. The resulting frames were then flat-fielded and stacked to create the final images which were finally flux calibrated using measurements of standard stars.

One advantage of the large number of foreground stars was that the relative positional alignment of the infrared and visible images could be accurately determined without using features within the galaxy itself.

Results

False-colour representations of the optical continuum and line images are shown in Figures 1–5 together with the overlayed K'(2.1 μm) isophotes and enlargements (× 5) of the nuclear region in the top right corners. Details are given in the captions. Note the small shift between the K' and optical continuum peaks which is about 2.5 σ of the residuals in the image alignment.

Line ratio images, produced by smoothing the line frames and including only the pixels where both lines were detected above 10 σ, are shown in Figures 6–7; the uniform dark blue zones represent regions with detected Hα+[NII] but with no [OIII] or [SII] emission within the above limits.

Contour plots of the IR broad band images are displayed in Figure 8 together

telescope. The K'(2.1 μm) image was obtained in July 1993 under photometric conditions but relatively poor seeing conditions (FWHM ≃ 1.6″) while the J and H observations were performed in June 1994 through thin cirrus but with better image quality (seeing FWHM = 0.9–1.0″). Data consisted of several pairs of object and sky frames plus dome flats with different levels of illumination. The scale in all images was 0.27"/pixel (lens LB of IRAC2) which provided an adequate field of view with proper sampling of the seeing disk.

For the data reduction sky images were first computed from the stack of sky frames (including removal of the back-

Figure 9: *Summary plot showing the relative locations of line and continuum features. The contours in the upper part are [OIII] and the enlarged view of the nuclear region shows the coronal [FeXI] line distribution and its location relative to both [OIII] and the K' continuum (nucleus). The insert in the upper right hand corner shows the relative displacements of the various line and continuum peaks. Note that all the visible peaks are displaced along the cone relative to the K' peak and that the [SII] (low ionization) line is strongest between the higher excitation [OIII] and [FeXI] line peaks.*

Peak positions
1: J (1.25 μm)
2: H (1.65 μm)
3: K (2.2 μm)
4: 5100 Å
5: 7000 Å
6: [Fe XI]
7: Hα+[N II]
8: [S II]
9: [O III]

with an enlargement of the central region which clearly shows that, although the nucleus is much more peaked in K' than in H and J, its position does not vary significantly with wavelength (the IR images are aligned within 0.2").

The relative positions of the central peaks in the various lines and continua are summarized in Figure 9 where we also include the contours of the [FeXI] coronal line image (see also O94). Note that, while the optical line/continua images are aligned within 0.04", the relative position of the IR peak is more uncertain ($\pm$ 0.2" 3σ) but sufficient to show a shift between the optical and IR continuum peaks.

A 'true-colour' line image (red = [SII], green = Hα+[NII], blue = [OIII]) is shown in Figure 10 where the structure of the cone and of the surrounding galaxy are best visible.

The nucleus

In the continuum at 5100 Å (Fig. 1) the emission is dominated by late B stars associated with an old starburst and extends over several arcsec with two spatially resolved peaks which are separated by 2" N–S but connected by a fainter bridge. The southern peak is coincident with the much more prominent 7000 Å nucleus (Fig. 2) which is single and unresolved. In the infrared (Fig. 8) the nucleus also shows only a single peak whose position is coincident at J, H and K' but which is more sharply peaked at K'. This infrared peak is also shifted by 0.25" relative to the southern visible peak in the direction away from the ionization cone (Fig. 9). We therefore assume that the 'true' nucleus is at or close to the position of the infrared peak and that the shift of the visible peak is an extinction effect. Extinction of the 'true' nucleus by $A_V \simeq 20$ magnitudes would be enough to hide it at 7000 Å but not at 1.25 μm and this value is close to that derived from the 9.7 μm silicate feature (Moorwood & Glass, 1984). The northern peak at 5100 Å shows faint Hα and [SII] emission, indicative of HII regions or supernova remnants, but its nature is unclear and we have proposed polarimetric imaging with HST to test if the visible 'nuclear' emission is dominated by scattered light.

The ionization cone

The galaxy shows a spectacular, one-sided [OIII] ionization cone (Fig. 3) whose asymmetry is probably due to extinction by the galaxy disk ($i \simeq 65°$) which also contains a prominent dust lane visible to the SE of the nucleus in the continuum images (Figs. 1, 2).
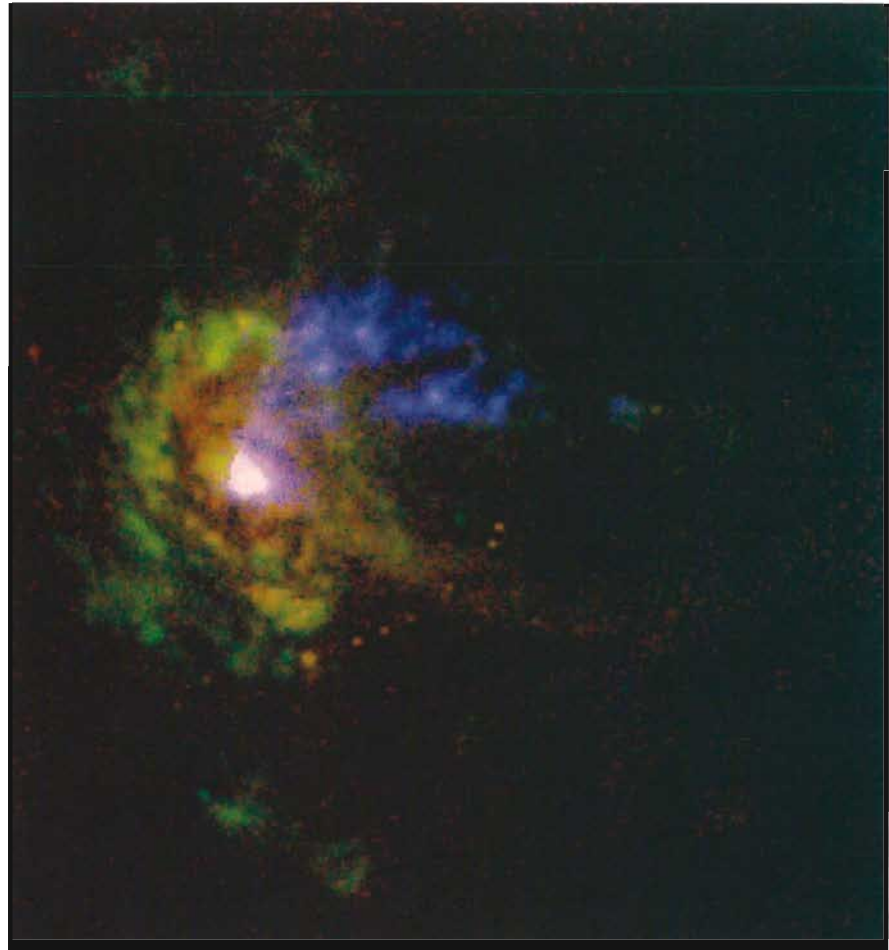

Figure 10: *A 'true colour' image of the Circinus galaxy with red = [SII], green = Hα+[NII] and blue = [OIII]. This representation clearly shows the ionization cone, the extended circumnuclear starburst and the chain of supernova remnants to the S.*

Within the cone there are high-excitation [FeXI] (see O94 for more details of the coronal line emission) and [OIII] clumps with observed [OIII]/Hα+[NII] > 2 (Fig. 6) or > 4 after correction for reddening. The relative positions of the various line and continuum peaks are shown in Figure 9. Both the intensities and spatial distribution of the high excitation lines can be modelled assuming photoionization by a power law spectrum and a suitably low gas density, i.e. $n_e \sim 40$ cm^{-3}, to obtain an ionization parameter $U \approx 0.01$. Pure photoionization models, however, cannot explain the simultaneous appearance of the prominent [SII] emission which peaks between [FeXI] and [OIII] and is coincident within 0.1" with the Hα + [NII] peak (Figs. 4, 5, 9) and reaches [SII]/Hα + [NII] ≥ 0.4 in some regions (Fig. 7). Our actual model which reproduces the high-excitation species predicts that [SII] should be produced about 0.4" beyond the [OIII] peak and pure photoionization models in general are unable to account for this reverse distribution regardless of the adopted nuclear ionizing continuum. A similar problem was found in a

detailed spectroscopic study of the extended NLR of NGC1068 (Bergeron et al. 1989). One possibility is that the [SII] knot is a photodissociating (or photoevaporating) molecular cloud with a large column density of freshly ionized gas leaving the cloud at sound speed ($\sim$10 km/s) which shields the rest of the material from soft ionizing photons but is transparent to X–rays ($h\nu > 100$ eV) which produce a large partially ionized region at the surface of the cloud.

We expect to obtain more detailed information on the relative roles of photoionization and other excitation mechanisms from visible (EMMI) and infrared (IRSPEC) spectroscopy scheduled at the NTT in March 1995.

The line emission outside the cone (P.A. < 10°) is typical of low excitation HII regions and is probably associated with the circumnuclear starburst described below.

Circumnuclear starburst activity

The Hα image (Fig. 4) clearly reveals the presence of a young starburst ($\leq 10^8$ yr) lying $\simeq 10"$ (200 pc) from the nu-

23

cleus and almost encircling it. Our supposition that the brightest extranuclear Hα emission is from normal HII regions is also supported by the very low values of [SII]/Hα+[NII] (Fig. 7).

Between the nucleus and the outer starburst there are regions with remarkably strong [SII] emission (Fig. 5) which most probably traces shocks from supernova remnants.

A remarkable feature is the series of 'spots' visible in the continuum and low-excitation lines (Figs. 1, 4, 5, 7 and 10) which are aligned along a chain $\simeq 20''$ south of the nucleus. These are the lowest excitation objects (i.e. those with the highest [SII]/Hα+[NII] ratio) which, together with their sizes ($\simeq 30$ pc), suggests that they are individual supernova remnants, possibly in small OB associations dominated by B stars. Additional spectroscopy and/or radio observations are needed to clarify their exact nature. As their orientation does not correspond to any obvious morphological feature we can only presume that they trace the location of a gaseous spiral feature in which starburst activity has already ceased.

Within the central $R \leq 2''$ (4 pc) the optical continuum images and the stellar absorption features observed in the optical and IR spectrum (Oliva et al. 1994, in preparation) are well fitted by a combination of late-B main-sequence stars and late K supergiants, i.e. typical of a starburst which is much older (many $\times 10^8$ yr) than the starburst ring.

The above results are consistent with a simple model in which a starburst propagates out of the nucleus. At the outer edge we see the most massive O stars from the latest generation (those photoionizing the HII regions) while closer inside less massive (early B) stars are still producing supernovae and remnants responsible for the [SII] emission. In the central regions (nucleus excluded) the high density of late B stars is responsible for the unusually blue colours while K supergiants dominate the near IR emission.

Conclusions

Line and continuum images of the Circinus galaxy have revealed a prominent ionization cone with coronal gas ([FeXI]) close to its apex and lower excitation [OIII] emission further out which is consistent with photoionization by a power law central source. Low excitation [SII] emission observed between the [FeXI] and [OIII] peaks, however, cannot be explained by pure photoionization models. This cone originates in a nucleus whose visible and infrared positions are spatially shifted suggesting that the true nucleus suffers $A_V \simeq 20$ magnitudes of extinction. Our observations are thus consistent with the presence of a torus which both obscures the Seyfert nucleus from direct view and collimates its UV continuum emission. In addition, a starburst ring which may or may not be related to the Seyfert nucleus is also present. Older starburst activity, which is perhaps more relevant to the possible evolutionary connection between starbursts and Seyfert activity, appears to have occurred closer to the nucleus. A puzzling discovery is the chain of compact, low excitation, objects $\simeq 20''$ S of the nucleus which are probably supernova remnants and associated B stars but require further study.

References

Antonucci, R., 1993, *ARAA*, **31**, 473.
Bergeron J., Petitjean P., Durret F., 1989, *A&A* **213**, 61.
Moorwood A.F.M., Glass I.S., 1984, *MNRAS* **135**, 281.
Oliva E., Salvati M., Moorwood A.F.M., Marconi M., 1994, *A&A* **288**, 457.

Multi-Wavelength Study of ROSAT Clusters of Galaxies

M. PIERRE, CEA/DSM/DAPNIA CE Saclay, France, and Max-Planck-Institut für Extraterrestrische Physik, Garching, Germany
R. HUNSTEAD, A. REID, G. ROBERTSON, University of Sydney, Australia
Y. MELLIER, G. SOUCAIL, Observatoire de Toulouse, France
H. BÖHRINGER, H. EBELING, W. VOGES, Max-Planck-Institut für Extraterrestrische Physik, Garching, Germany
C. CESARSKY, J. OUKBIR, J.-L. SAUVAGEOT, L. VIGROUX, CEA/DSM/DAPNIA CE Saclay, France

1. Clusters of Galaxies as Cosmological Probes

Among the 60,000 X-ray sources detected by the ROSAT All-Sky Survey, about one tenth are expected to be clusters of galaxies. This represents a considerable potential for cosmological studies and has motivated numerous identification campaigns, especially at ESO; we describe here such a programme together with associated observations at other wavelengths.

As the most massive bound entities known in the universe, clusters of galaxies are key objects for testing the predictions of the various cosmological scenarios. They originated from the highest peaks in the initial density fluctuations, and are expected to have evolved through characteristic processes, namely, "top-down" or "bottom-up" depending on the nature of the dark matter ("hot" or "cold"). Practically, these alternatives correspond to situations in which clusters formed either from the fragmentation of large "pancakes" or from the merging of sub-groups, and should ideally be reflected in the evolution of the cluster mass function. While the mass of a cluster is not a directly observable quantity, a number of other physical parameters can be measured directly and, therefore, provide a detailed picture of the dynamical cluster environment as a function of redshift.

2. Observational Tests

Relevant observations of clusters encompass the whole electromagnetic spectrum; a short overview includes: